Self-inflating floating nanofiber membranes for controlled drug delivery

Serdar Tort[a,b], Daewoo Han[a], Andrew J. Steckl[a,*]

[a] Nanoelectronics Laboratory, Electrical Engineering and Computer Science, University of Cincinnati, Cincinnati 45221-0030, USA
[b] Department of Pharmaceutical Technology, Faculty of Pharmacy, Gazi University, Ankara 06330, Turkey

ABSTRACT

Floating gastro-retentive delivery systems can prolong the gastric residence providing sustained drug release. In this study, we report on self-inflating effervescence-based electrospun nanofiber membranes embedding polyethylene oxide/sodium bicarbonate cast films. In this system, sodium bicarbonate results in an effervescence effect by creating carbon dioxide gas upon contacting an acidic gastric fluid, with the resulting gas bubbles being entrapped within the swollen network of nanofibers. Eudragit RL and RS polymers are utilized as a host material to manipulate release kinetics of incorporated drugs. Pramipexole, a common medication for chronic Parkinson's disease (PD), is used as a model drug. Uniform and bead-free nanofibers with diameters of ~300 nm were obtained. Although floating nanofibers initially exhibited high water contact angles (WCA), water droplets were quickly absorbed into the surface and the WCA decreased to ~0° within 60 s. Floating lag time, total floating time, swelling properties and drug release profiles were investigated both in a simulated gastric fluid (pH 1.2 buffer solution) and in a simulated intestinal fluid (pH 6.8 buffer solution) at 37 °C. All floating nanofiber formulations began to float instantly with nearly zero floating lag time and did not sink into the solution even after 24 h. By comparison, the same formulations without sodium bicarbonate cast films could not maintain continuous floating beyond 15 min. The floating nanofiber pouches presented lower initial release of between 20 and 57 %, compared to that of non-floating nanofiber pouches (40–82% within 2 h). Clearly, floating nanofibers reduced the initial burst release and provided sustained drug release. This demonstrates the potential to result in 'once-a-day' oral introduction of drugs that normally must be taken frequently. Effervescence-based floating nanofibers present a novel and promising prototype delivery system for the drug delivery in the upper gastro-intestinal (GI) tract.

1. Introduction

Oral drug delivery is the preferred route of drug administration because of its noninvasive nature, ease of use, higher patient compliance and cost-effectiveness (Viswanathan et al., 2017). Oral drug delivery with controlled release kinetics is effective for chronic diseases with frequent dosage consumption. To reduce the drug concentration below the toxic level in plasma, controlled drug delivery systems can be approximated by multiple administrations of immediate release formulations (Moodley et al., 2011). An important controlled drug delivery system in oral formulations is the gastro-retentive delivery system (GRDS) (Malik et al., 2015a; Singh, 2000; Streubel et al., 2006). The use of GRDS can resist contractions and peristaltic waves in the stomach and show the sustained release of drugs in the gastric environment (Awasthi and Kulkarni, 2016). Therefore, increasing the gastric residence time of some drugs that are stable at the acidic pH in the stomach or upper GI tract could increase their bioavailability. For some drugs, such as baclofen and metformin HCl, their main principal sites of drug absorption are either the stomach itself or the upper part of small intestine and these drugs are significantly degraded in the colon. Therefore, the gastric retention property is highly beneficial to deliver those drugs for an extended time period (Mandal et al., 2016). Approaches for GRDS development include the floating drug delivery system (FDDS) or the non-floating system (mucoadhesive, swelling, or high-density systems). FDDS can be developed (Reddy et al., 2013) either by an effervescent or a non-effervescent system (hydrodynamical system, alginate beads or matrix layered tablets). While the non-effervescent FDDS uses a swelling system, the effervescent FDDS is formulated such that when in contact with the acidic gastric fluid (pH of ~1.5–3), CO_2 gas is generated and becomes entrapped in swollen hydrocolloids, providing buoyancy to the dosage form (Singh, 2000).

Fibers with homogenous or complex structures formed by the electrospinning method have been reported to provide excellent controlled release of drugs and other functional molecules (Han et al.,
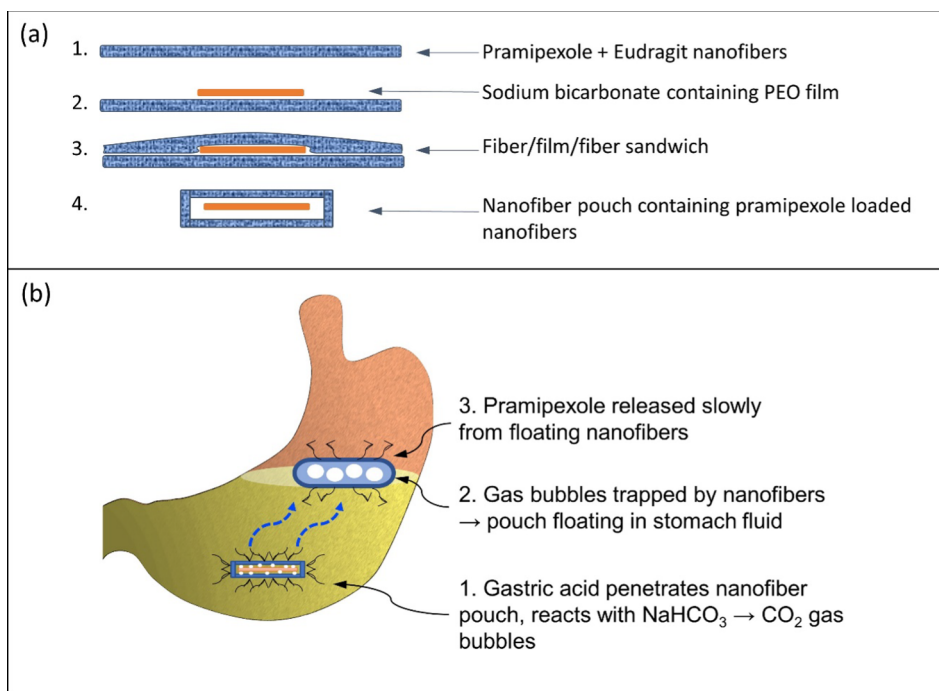
Fig. 1. Floating nanofiber pouch: (a) preparation process for PEO/NaHCO$_3$ film embedded nanofiber pouch; (b) basic mechanism for sustained pramipexole drug delivery in stomach using floating nanofiber pouch.

2017; Han and Steckl, 2013; Hu et al., 2014; Palo et al., 2017). With the growing interest in the development of new electrospinning methods (including coaxial, triaxial and side-by-side electrospinning), nanofibers providing controlled release with many different mechanisms have been produced (Jiang et al., 2014; K. Wang et al., 2018; Yang et al., 2016; Yu et al., 2016). Electrospun nanofiber membranes have a microporous structure that is sufficiently small, such that when they swell quickly they trap generated gas within the membrane. In addition to many advantages for drug delivery systems, electrospun nanofibers provide specific benefits (Malik et al., 2015a) for developing an effervescent FDDS because (a) gastric fluid can reach the embedded sodium carbonate-PEO film through pores; (b) generated CO$_2$ gas is not able to diffuse out from the nanofiber system, resulting in the flotation of drug-incorporated nanofiber pouches (Fig. 1) (Adibkia et al., 2011). Electrospun nanofiber membranes are promising systems for oral drug delivery to provide sustained, dual or site-specific drug release profiles (Hamori et al., 2014; Karthikeyan et al., 2012; Shahriar et al., 2019; Wang et al., 2015). Several nanofiber-based drug delivery systems have been developed to keep nanofibers in the stomach for a sustained drug release (Darbasizadeh et al., 2018; Malik et al., 2015; Suvannasara et al., 2014). For example, nanofibers containing tripolyphosphate (TPP)-crosslinked chitosan/poly(ethylene oxide) - ranitidine hydrochloride were produced as a FDDS (Darbasizadeh et al., 2018). The prepared nanofibers remained floating for more than 24 h and released ~70% of drug at an acidic pH. In another study, Malik et al. produced a diacerein-loaded gastro-retentive nanofiber system using poly L-(lactic acid) (Malik et al., 2015). They reported that 61.3% of the drug was released in 30 h at an acidic pH. Chitosan was also used to prepare mucoadhesive nanofibers for gastric retentive drug delivery in acidic conditions (Suvannasara et al., 2014).

Different types of Eudragit polymers have been developed that dissolve in specific pH conditions and thus can release drug in targeted locations of the GI system. For the targeted drug delivery in different segments of the GI tract, electrospun fiber membranes have been developed using various types of Eudragit polymers (Han et al., 2017; Jin et al., 2016; Shen et al., 2011; Turanli et al., 2019). Eudragit RL and RS polymers consist of poly (ethyl acrylate, methyl methacrylate,

trimethylammonium-ethyl methacrylate chloride) with the ratio of 1:2:0.2 and 1:2:0.1, respectively. Increasing the amount of quaternary ammonium groups renders the polymer network more hydrophilic and the mobility of water molecules within the polymer network is increased (Glaessl et al., 2010). Eudragit RL and RS polymers are insoluble in acidic digestive fluids but are permeable and show pH-independent swelling properties. Eudragit RS contains 5% hydrophilic quaternary ammonium groups, while Eudragit RL has 10% ammonium groups, which makes Eudragit RL more permeable. Mixture of these polymers in different ratios can achieve the desired release profiles. Eudragit polymers are used in various formulations, such as tablet (Qiao et al., 2010), pellet (Elsamaligy and Bodmeier, 2015), film (Gryczke et al., 2011), nanoparticle (Hoobakht et al., 2013), microsphere (Adibkia et al., 2011), microsponge (Jain and Singh, 2010) and nanofiber (Dwivedi et al., 2018), in order to provide the sustained or delayed release of drugs. Eudragit RS-PO, EPO and L polymers have been also used in floating tablet and bead studies (Bani-Jaber et al., 2011; Fukuda et al., 2006; Huanbutta et al., 2017).

Pramipexole (PPX) is a selective dopamine D$_2$ sub-family receptor agonist, specifically the dopamine D$_3$ receptor, and is an FDA approved drug for the treatment of Parkinson's disease (PD). PPX is administered as a monotherapy in the early stage of PD and as an adjuvant therapy for advanced PD cases. PPX has an absolute bioavailability > 90%, with a half-life of ~8 h, which undergoes little presystemic metabolism and reaches peak concentrations in 2 h. PPX has been reported to be quite stable under acidic conditions (Pawar et al., 2013) and foods do not affect the extent of PPX absorption in the GI tract. Therefore, PD patients are required to take the immediate release formulation three times a day (every 8 h). In many cases, this results in missing doses during chronic therapy. To overcome this problem, controlled release formulations of PPX have been developed (Jenner et al., 2009). Recently, studies have reported on the use of PPX nanocrystals for transdermal permeation and a PPX prolonged delivery system using nanoparticles (Li et al., 2018; Y. Wang et al., 2018). These studies aimed to provide consistent sustained delivery of PPX, eliminating the fluctuation of the drug level in the blood. Long lasting formulation of PPX could prevent the sudden and uncontrolled release of the drug and

dose dumping (Eisenreich et al., 2010).

To date, there is no report on PPX-containing nanofibers. Although an extended release tablet containing PPX is available in the market, a nanofiber platform provides versatile options to incorporate multiple drugs and/or enable stimulus-triggered delivery by adapting more complex materials and structures, such as coaxial or triaxial fibers. To date, only a few studies on floating properties of nanofibers have been reported and they do not utilize gas generation (non-effervescent) (Darbasizadeh et al., 2018; Malik et al., 2015). Moreover, these studies were performed in steady state conditions without mechanical stimulation that would simulate gastric movements. Here we report a novel and promising nanofiber-based effervescent approach for producing floating nanofibers by embedding a polyethylene oxide (PEO)/sodium bicarbonate ($NaHCO_3$) film, which releases CO_2 gas in the stomach upon reaction with gastric acid. This is a prototype delivery system for drugs that are locally effective in the stomach or absorbed in the stomach or upper GI tract. PPX has a broad range of dosages for once daily treatments, ranging from ~0.4 to 4.5 mg depending on the severity of symptoms in chronic PD treatments. The drug amount loaded in the nanofiber membrane is readily adjustable by manipulating the electrospinning process time or drug concentration (Shao et al., 2015). Therefore, this system is suitable to produce personalized floating drug delivery systems for PD patients. The basic concept is illustrated in Fig. 1b. Briefly, when the floating nanofibers reach the stomach, gastric acid penetrates into the nanofiber membrane and reacts with the PEO/$NaHCO_3$ film. Drug molecules are released from nanofibers while CO_2 gas is generated and trapped inside membrane.

2. Materials and methods

2.1. Materials

PPX dihydrochloride monohydrate (98%), $NaHCO_3$, dimethyl sulfoxide (DMSO), ethanol and methanol were purchased from Fisher Scientific (Pittsburgh, PA). Polyethylene oxide (PEO, Mn 1000 kDa), and poly(vinyl alcohol) (PVA) were purchased from Sigma Aldrich (St. Louis, MO). Polyvinylpyrrolidone (PVP, Mw 1300 kDa) and N,N-dimethylacetamide (DMAc) were purchased from Acros Organics (Geel, Belgium). Eudragit RL 100 and RS 100 were generously supplied by Evonik Chemicals (Essen, Germany). All chemicals used in buffer solutions and electrospinning solutions are reagent grade.

2.2. Preparation of PEO/$NaHCO_3$ films

Because electrospinning with highly concentrated $NaHCO_3$ solution was challenging, $NaHCO_3$ was incorporated into thin PEO cast films (Fig. 2a) to generate gas bubbles in acidic gastric fluid (Fig. 2b). Different polymers, such as PVP, PVA, and PEO were tested to produce $NaHCO_3$-incorporated films and nanofibers. However, because of the acidity of prepared 6% (w/v) PVP solution (pH ~ 4.3), added $NaHCO_3$ generated gas bubbles immediately in PVP solution. Thus, the PVP/$NaHCO_3$ film loses its ability to generate gas when it is used for actual drug delivery. PVA was also not dissolved in $NaHCO_3$ containing solution. Eventually, PEO was selected for this purpose because it dissolves without affecting $NaHCO_3$ in solutions (pH of 6% PEO solution ~ 8.4). Prepared solutions containing 6% PEO and 2% $NaHCO_3$ were homogenized in a rotating stirrer for 24 h. Homogenized solution was cast on a glass slide and then dried for 24 h at room temperature. The dried cast films were cut with a circular metallic die (3 mm diameter) and stored in a nitrogen purged desiccator until used for incorporation into electrospun membranes.

2.3. Preparation of floating nanofibers

Floating nanofiber membranes were produced by the electrospinning method. To control the PPX release kinetics, Eudragit RL and RS

mixture were chosen as polymer hosts. The total polymer concentration in electrospinning solutions was fixed at 20% in all cases, while the ratio between Eudragit RL and RS was varied to manipulate the release kinetics. Eudragit polymers and PPX were dissolved in ethanol:methanol:DMAc:DMSO (8:6:3:3) solvent mixture using a rotating stirrer for 24 h. Although PPX has better solubility in methanol than ethanol, ethanol improves the electrospinnability of Eudragit polymer solutions. To prevent clogging of the nozzle and maintain the drug solubility, DMAc and DMSO were added, allowing continuous electrospinning process (Shen et al., 2009). In order to eliminate the effect of process parameters on nanofiber properties, the various formulations with different Eudragit polymer types and their ratios (Table 1) were prepared using the same electrospinning parameters: 12 kV applied bias, a needle-tip to collector distance of 15 cm, and a flow rate of 0.15 mL/h. After electrospinning 500 μL of the polymer solution, previously prepared 3 mm diameter PEO/$NaHCO_3$ circular cast films were placed on the electrospun nanofiber membrane and then the electrospinning process was continued until an additional 500 μL of polymer solution was electrospun on top (Fig. S1) so that PEO/$NaHCO_3$ films were completely embedded inside nanofiber membranes (Fig. 2c). In this approach, PEO/$NaHCO_3$ film embedded nanofiber membranes (Fig. 1a) were obtained without using a molding process (Park et al., 2011). The overall process shown schematically in Fig. 1a illustrates how the PEO/$NaHCO_3$ film is sandwiched by fiber membranes during the electrospinning process. PEO/NaHCO3 film embedded nanofiber pouches were prepared after cutting the membrane into circular pieces with diameter of 9 mm. Different formulations that were investigated are listed in Table 1. F1, F2 and F3 contain PEO/$NaHCO_3$ films, while F4, F5 and F6 have no PEO/$NaHCO_3$ films. In the acidic condition, the difference between activated PEO/$NaHCO_3$ film containing and non-containing nanofiber membranes can be clearly seen on Fig. 2d.

2.4. Characterization of floating nanofibers

2.4.1. Scanning electron microscopy (SEM) images

SEM images were obtained with Scios DualBeam SEM (Thermo Fisher Scientific) at an acceleration voltage of 5 kV to observe the morphology of nanofibers. All samples were sputter-coated with gold/palladium to prevent charging issues during SEM observation. After SEM imaging, the mean diameter of formulations was analyzed using ImageJ software (National Institutes of Health, USA) on 50 different nanofibers for each sample.

2.4.2. Fourier-transform infrared (FTIR) spectroscopy, differential scanning calorimetry (DSC) and X-Ray diffraction (XRD) studies

Individual characteristic XRD peaks of pure PPX, Eudragit RL, Eudragit RS and their composite nanofibers were obtained in order to determine any incompatibility between polymers and PPX. FTIR spectra (average of 32 scans) were obtained by using an FTIR spectrometer (Thermo Scientific, Nicolet 6700) on a diamond ATR Smart Orbit probe in the range of 4000–400 cm^{-1}.

Thermal analyses of pure PPX, Eudragit RL and RS and their composite nanofibers were evaluated using DSC (TA Instruments, Discovery DSC2500). The samples were accurately weighted (~2 mg), placed in an aluminum pan and sealed with lids. DSC thermograms were achieved at a heating rate of 10 °C/min from 40 to 200 °C under nitrogen atmosphere, with an empty pan being used as reference.

XRD studies were performed to evaluate the physical form (crystalline or amorphous) of drug, polymers and nanofibers. XRD patterns were recorded over the 2θ range from 10 to 35° with the scan rate of 0.05°/min and a step time of 0.5 s/step using Philips X'Pert MPD diffractometer with Cu Kα-radiation.

2.4.3. Wettability studies

To characterize the surface hydrophilicity, the water contact angle (WCA) of nanofibers was measured with an optical tensiometer (First
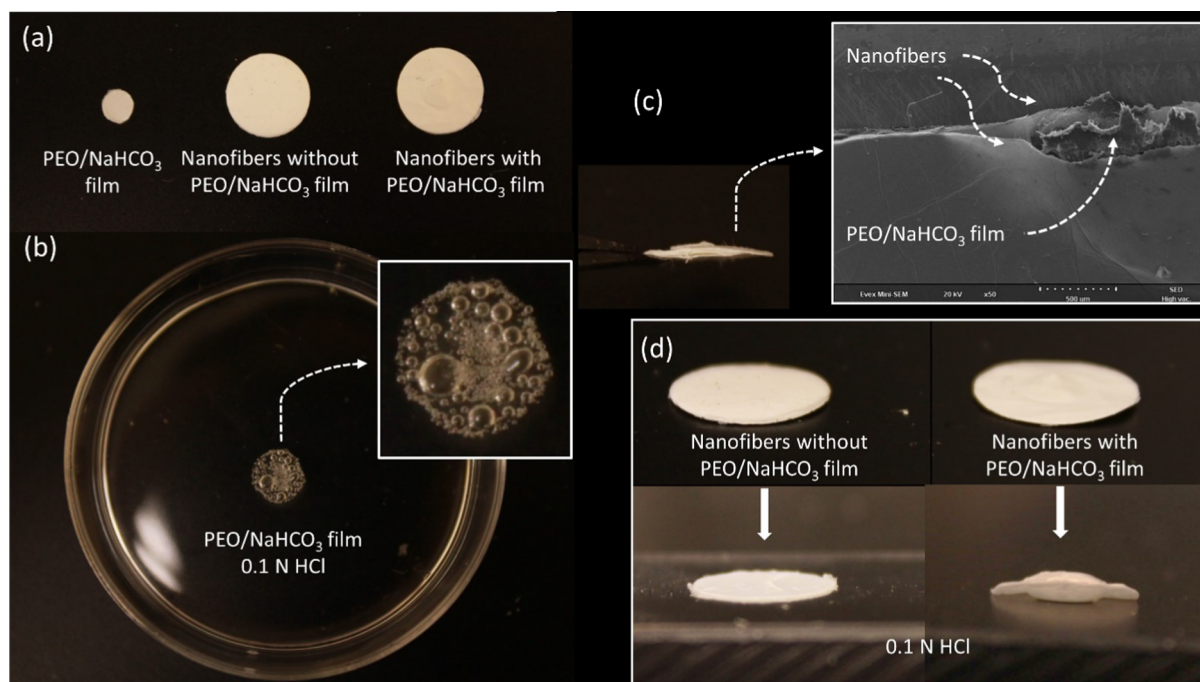
Fig. 2. Photographs of floating nanofiber delivery system: (a) PEO/NaHCO$_3$ film (left) and nanofiber membranes without (middle) or with (right) embedding PEO/NaHCO$_3$ film; (b) air bubble generation from PEO/NaHCO$_3$ film in 0.1 N HCl; (c) cross-section of nanofiber membranes embedding PEO/NaHCO$_3$ film; (d) nanofiber pouches without (left) and with (right) PEO/NaHCO$_3$ film before (top) and after (bottom) activation in 0.1 N HCl.

Table 1
Formulations of nanofibers with different Eudragit compositions.

Formulation Code	Eudragit RL100 %	Eudragit RS100 %	PPX %	PEO/NaHCO$_3$ film
F1	20	–	0.2	O
F2	10	10		O
F3	–	20		O
F4	20	–		X
F5	10	10		X
F6	–	20		X

Ten Angstroms, 1000 B Drop Shape Instrument). Distilled water droplets of 5 μL were placed on different nanofiber surfaces and the contact angle between the surface and the water droplet was measured. An average WCA was calculated from three measurements.

2.4.4. Swelling index

Although Eudragit RL and RS are water insoluble polymers, they are pH-independent swellable and permeable polymers (Thakral et al., 2013). Therefore, the swelling index of Eudragit nanofibers is significant for an approximation of sustained drug release. Swelling ratios of nanofibers were determined via the gravimetric method in acidic conditions at 37 °C for 24 h. The swelling index was calculated at different time points by determining the ratio of the increased weight of wet nanofibers to the weight of dry nanofibers, as shown in Eq. (1). Excess buffer solution on the surface of the nanofibers was removed using an absorbent before weighing.

$$Swelling\ index\ (\%) = \frac{(m_{final} - m_{initial})}{m_{initial}} \times 100 \tag{1}$$

2.4.5. Floating lag time and total floating time studies

Floating lag time (FLT) and total floating time (TFT) are defined as the duration that the immersed nanofibers into the buffer solution require to rise to the solution surface and the time period of continuous floating on the gastric fluid surface, respectively. To measure FLT,

nanofibers were placed on the bottom of a beaker. Then, simulated gastric fluid (50 mL of 0.1 N HCl) at 37 °C was poured and stirred at 75 rpm using magnetic bar to mimic the gastric conditions (Baldaniya et al., 2015; Fukui et al., 2017). All times were measured using a stopwatch and performed in triplicate (n = 3).

2.4.6. In vitro drug release studies and kinetic modelling

To determine the floating effect on drug release kinetics, *in vitro* drug release studies were carried out using formulations with (F1, F2, F3) and without (F4, F5, F6) PEO/NaHCO$_3$ films. Drug release studies were carried out at 37 °C for up to 24 h in both 0.1 N HCl simulated gastric fluid and in pH 6.8 buffer solution. Optical absorption spectra were taken at predetermined time intervals and the amount of PPX was measured optically at 264 nm. The drug release profiles were analyzed with DDSolver software to obtain the best fit kinetic models (Zhang et al., 2010). The release constant and correlation coefficients of various kinetic models were calculated.

2.5. Statistical analysis

The statistical analysis of the characterization study (wettability study, swelling index) results were executed using the Statistical Package for the Social Sciences (SPSS) version 21. The significance of differences between data sets was tested with one-way analysis of variance (ANOVA) and Tukey post-hoc test. The p values < 0.05 were considered statistically significant. For comparison, the *f1 difference factors* were calculated for release profiles of floating and non-floating formulations using the DDSolver software.

3. Results and discussion

3.1. Scanning electron microscopy (SEM) images

Electrospinning is a very rapid and sensitive production method and process parameters mostly affect nanofiber properties. Zhou et al. reported (Zhou et al., 2019) that increasing the applied voltage decreased the length of the stable (straight) liquid jet and increased the spreading
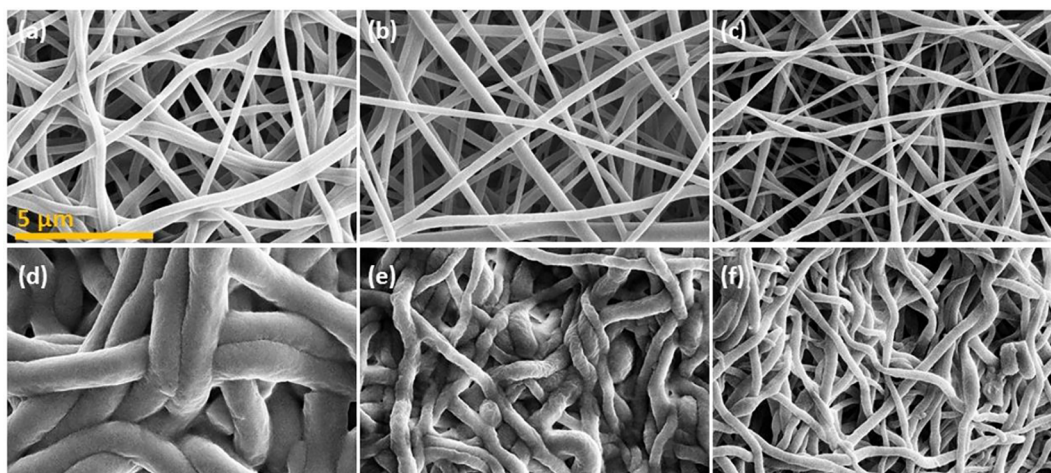
Fig. 3. SEM images of fiber morphologies: (a) F1, (b) F2, and (c) F3 nanofibers before hydrating in acidic medium; (d) F1, (e) F2, and (f) F3 nanofibers after 24 h hydration in pH 1.2 acidic medium. All images are shown in the same scale.

angle of the bending and whipping regime, which in turn resulted in reduced nanofiber diameter and faster drug release. Similarly, the distance between nozzle tip and collector and the flow rate of polymer solutions can affect the nanofiber structure. Therefore, we kept the process parameters constant for all formulations. As seen in SEM images (Fig. 3), the electrospun fibers formulations all have smooth and uniform surfaces. The mean fiber diameters of F1, F2, F3 formulations were found to be 314 ± 90, 295 ± 42 and 241 ± 59 nm, respectively. Addition of Eudragit RS polymer decreased the nanofiber diameter and increased the rigidity of nanofibers, leading to brittleness and some breakage of nanofibers when peeling off from the aluminum foil after electrospinning. SEM images of nanofiber samples that had been placed in acidic (pH 1.2) solution for 24 h were taken to investigate the effects of the acidic medium on the nanofiber structure. After 24 h in the acidic condition, the nanofiber structure of F1 formulation (Fig. 3d), which contains only Eudragit RL as polymer, presented more dramatic changes in fiber diameter than F2 and F3 formulations (Fig. 3e–f), because Eudragit RL is more hygroscopic with higher swell index compared to Eudragit RS. The mean diameter of F1 nanofibers increased to 1321 ± 100 nm, while the mean diameter of F2 and F3 nanofibers increased to 495 ± 81 nm and 354 ± 57 nm, respectively. Higher Eudragit RS concentration resulted in smaller increase of fiber mean diameter due to low swelling property compared to Eudragit RL.

3.2. FTIR/DSC/XRD studies

FTIR spectra of PPX, Eudragit RL, RS and their composite nanofiber formulations are shown in Fig. 4a. The FTIR spectrum of PPX showed characteristic peaks at 3410 cm^{-1} from N−H stretching, 2942 cm^{-1} from aromatic C−H stretching, 1630 cm^{-1} from amide I band, 1585 cm^{-1} from C=C stretching, and 1070 cm^{-1} from N−C stretching. Eudragit RL and RS have characteristic peaks at 2950 cm^{-1}, 1722 cm^{-1} and 1141 cm^{-1} corresponding to the C−H, C=O and C−O−C stretching, respectively. The characteristic peaks of PPX and Eudragit polymers are in accordance with the literature (Gianak et al., 2018; Muthu et al., 2013). It was not possible to observe the N−H and aromatic C−H stretching peaks of PPX due to overlap with the C−H stretching peak of Eudragit polymers. The characteristic N−C and C=C stretching peaks of PPX were observed with reduced intensity in the F1, F2 and F3 spectra, as shown in Fig. S2. These results show that intact PPX molecules were present in nanofibers and no spectral change of the characteristic absorption bands of PPX and polymers occurred due to chemical or physical reaction.

PPX has a melting point at 280–300 °C with decomposition and does not have a sharp endothermic melting peak. To avoid the decomposition of PPX at the melting point, DSC studies were performed below the melting point (Papadimitriou et al., 2008). PPX shows an endothermic peak at 105 °C related to the evaporation of water, which indicated a partial crystalline nature of PPX (Bahari Javan et al., 2018) (Fig. 4b). This endothermic peak could not be observed in nanofiber thermograms due to the complete entrapment of PPX within nanofibers, the rapid evaporation of the solvent during the electrospinning, or the conversion from the crystalline state to amorphous state by the high electrospinning voltage (Reda et al., 2017).

The XRD study was used to identify the physical form of the drug in nanofibers. Significant distinct diffraction peaks were observed at 12.03°, 21.38°, 24.23°, 24.78°, and 28.48° for the PPX-only indicating the crystalline form of the drug (Papadimitriou et al., 2008) (Fig. 4c). No such peaks were detected in either the Eudragit polymers or in the nanofibers, indicating an amorphous PPX structure (Fig. 4c) that confirms the DSC results.

3.3. Wettability studies

When the nanofiber-based FDDS reaches the stomach, the embedded PEO/NaHCO$_3$ film should be timely dissolved to create gas bubbles in a gastric fluid, providing the floating function. Therefore, sufficient wettability of the floating nanofiber pouch is a critical property because the PEO/NaHCO$_3$ film cannot generate gas bubbles without contacting the acidic fluid through membranes. The WCAs of F1, F2 and F3 at the initial measurement were found to be 115°, 121° and 124°, respectively (Fig. 5). Increasing Eudragit RS concentration increased the contact angle due to the hydrophobic nature of Eudragit RS. Santocildes-Romero et al. reported (Santocildes-Romero et al., 2017) that the addition of Eudragit RS to PVP nanofibers increased the WCA from 0° to 127°. In our study the WCA of all formulations gradually decreased to 0° within 60 s after placing the water droplet, confirming the good permeability of these membranes (Fig. 5). The contact angle values decreased significantly for each time point ($p < 0.05$). The wettability study indicated that the nanofiber membrane formulations have suitable surface properties to dissolve the embedded PEO/NaHCO$_3$ film.

3.4. Swelling index

Eudragit RL and RS are pH-independent polymers with different swell index and permeability, which makes them suitable for sustained release applications. Combining these polymers in different amounts can produce a desired release profile, where drugs are diffused through
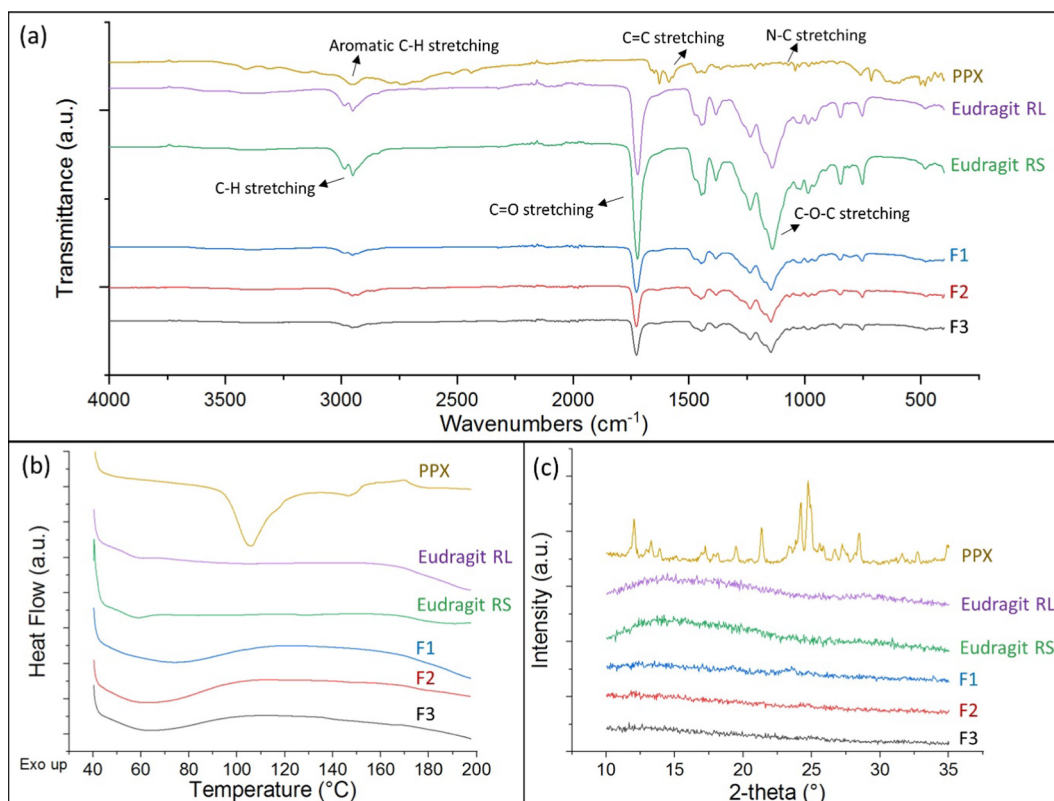
Fig. 4. Material characteristics: (a) FTIR spectra of pure PPX, Eudragit RL, RS and F1, F2, F3 nanofiber formulations; (b) DSC thermograms of pure PPX, Eudragit RL, RS and F1, F2, F3 nanofiber formulations; (c) XRD diffractograms of pure PPX, Eudragit RL, RS and F1, F2, F3 nanofiber formulations.
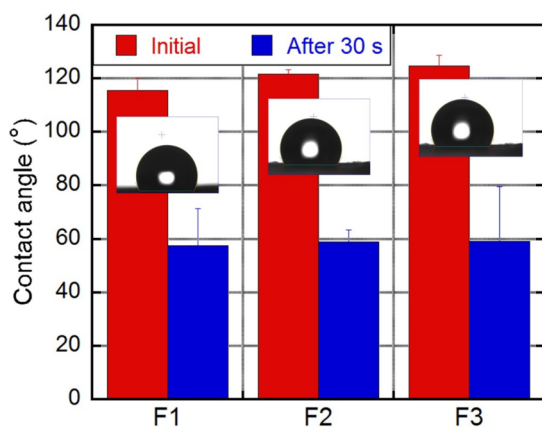

Fig. 5. Water contact angle values of F1, F2, and F3 nanofiber membranes embedding PEO/NaHCO₃ films: at initial and at 30 s values. All water droplets were fully absorbed at ~60 s.

Fig. 6. Swelling index values of nanofiber formulations at different time points (n = 3; *$p < 0.05$).

the hydrated polymer matrix. The swelling indices of formulations are shown on Fig. 6. The formulation containing Eudragit RL-only (F1) had the highest swelling index of 287% after 24 h in the solution. The nanofiber formulation with 1:1 Eudragit RL and RS blend (F2) decreased the swelling index to 212%, while the Eudragit RS-only formulation (F3) had the lowest swelling index of 183%. When the intra-group data were evaluated for each formulation, there was no significant difference between the swelling index values at different time points. When the swelling indices were compared between formulations, a significant difference was only found between F1 and F3 at the 8th hour point ($p < 0.05$). As expected, the swelling index of Eudragit RS was found to be less than Eudragit RL, because fewer water molecules diffused into the polymer network. These results are consistent with SEM images of
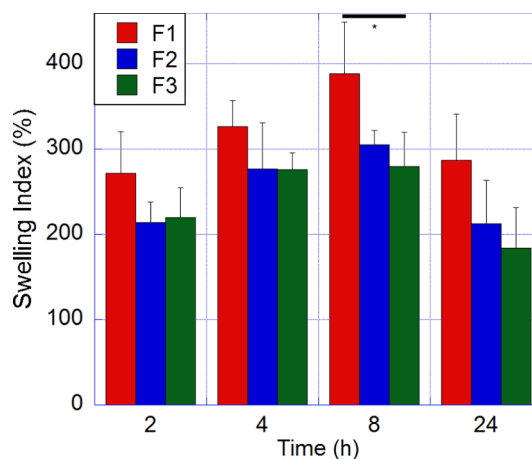
fiber membranes (Fig. 3d–f). Glaessl et al. reported (Glaessl et al., 2010) that water acts as a plasticizer for Eudragit polymers. Therefore, the Eudragit RL formulation has greater expansion ability without losing its integrity. Akhgari and Tavakol reported (Akhgari and Tavakol, 2016) that films containing Eudragit RS and RL had a swelling index between 12.9 and 39.8 % in acidic solution. The higher swelling index values in our study are due to interconnected fibrous pores and higher surface area of the nanofiber membranes. As shown in Fig. 6, the swelling index of all formulations increased until the 8 h time point, while at 24 h the value had decreased to a level similar to that after 2 h. Misra et al. reported (Misra et al., 2017) a similar trend with Eudragit containing nanofibers, which they attributed to the degradation of integrity of polymeric nanofibers in simulated body fluid.

3.5. Floating lag time and total floating time studies

Gastric retentive drug delivery systems require short FLT and long TFT values. FLTs for all nanofiber formulations were very short (< 1 s), including for the PEO/NaHCO$_3$ film-free formulations (F4, F5 and F6). The main reason for the fast FLT is the high surface area-to-volume ratio of nanofibers, resulting in an effective bulk density lower than the gastric fluid density (1.003 g/cm^3) (Malik et al., 2015a). Once the membrane pouch containing the PEO/NaHCO$_3$ film is completely wet in the acidic solution, the PEO/NaHCO$_3$ film generates gas bubbles inside. Thus the F1, F2 and F3 formulations have more than 72 h TFT values, while F4, F5 and F6 were completely immersed in the solution within 15 min (Fig S3). Formulations without PEO/NaHCO$_3$ films (F4, F5, F6) could not maintain floating properties in gastric environment conditions. Similarly, formulations with PEO/NaHCO3 films (F1, F2, F3) also showed no floating effect in basic buffer solution due to no gas generation. The time required for generating a CO$_2$ gas pocket within F1, F2 and F3 was ~3 min, which is shorter than the sinking time of F4, F5 and F6. F1, F2, and F3 nanofiber pouches can maintain their buoyancy over 24 h. Previous FLT and TFT studies have been reported without (Gambhire et al., 2007; Pawar and Dhavale, 2014) and with (Eberle et al., 2014; Thapa and Jeong, 2018) and solution agitation by rotation. Although some studies have reported (Darbasizadeh et al., 2018; Malik et al., 2015) that a nanofiber system can float without gas generation, no mechanical actions were applied during FLT and TFT measurements, which does not fully simulate the actual gastric motility environment.

3.6. Drug release studies and kinetic modelling

To determine the difference in drug release behavior between floating (F1, F2, F3) and non-floating systems (F4, F5, F6), studies were carried out with all six formulations in 0.1 N HCl. The release behavior of floating nanofibers in pH 6.8 buffer solutions was also evaluated to determine the release kinetics in the intestine. The results are shown in Fig. 7. For all cases, Eudragit RS decreased the burst release and retarded the release of PPX compared to that of Eudragit RL, providing a sustained drug release in acidic conditions. In addition, all floating formulations showed sustained drug release compared to non-floating formulations, as seen by comparing the results in Fig. 7a and b. Eudragit RS is a less permeable polymer than Eudragit RL due to the presence of fewer quaternary groups, leading to a slower drug release. These results are consistent with the swelling index results. More water permeable polymer structures increased both the swelling index and the release rate. In Fig. 7d, the F4 formulation showed a burst PPX release (67%) at 30 min, while the F1 formulation provides a reduced burst release of ~40%. In addition, the F1 formulation released 90% of PPX in 24 h, while the F4 formulation quickly released 90% of PPX in only 4 hr.

All floating formulations showed a more sustained release profile of PPX with lower burst release, compared to non-floating formulations (Fig. 7d–f). Although the burst release of drug molecules can be reduced by using coaxial or triaxial nanofibers, we have used homogenous nanofibers that are simpler to produce (Yu et al., 2015). Obviously, the floating mechanism retarded the drug release successfully. The F5 formulation quickly released 60% of PPX in 90 min, while the F2 released 60% in 16 h, which is more than $10 \times$ longer duration (Fig. 7e). Similarly, the F6 formulation released 60% of PPX in 7 h, while the F3 released 60% in 24 h (Fig. 7f). It was possible to increase the amount of drugs released by increasing the Eudragit RL concentration. The *f1 difference factors* of F1-F4, F2-F5 and F3-F6 formulations were found to be 45.71, 55.24 and 34.62, respectively. For all cases, the *f1 difference factor* was found to be higher than 15, which clearly indicated dissimilarity between formulations. As expected, the PPX release rate from nanofibers in pH 6.8 buffer solution (Fig. 7c) was faster than in the acidic condition (Fig. 7a). As expected in basic conditions, there was no floating effect and hence no sustained release of PPX is observed. Lee et al. reported (Lee et al., 2017) that chloride anions are less selective to ion exchange at pH 1.2 than phosphate cations at pH 6.8. The degree of hydration and the permeability of the polymer matrix decreases in acidic conditions, leading to a quicker release in basic conditions.

According to the observed release profiles, the PEO/NaHCO$_3$ films provide nanofiber membrane formulations a floating effect and more sustained drug release profiles than membranes without PEO/NaHCO$_3$
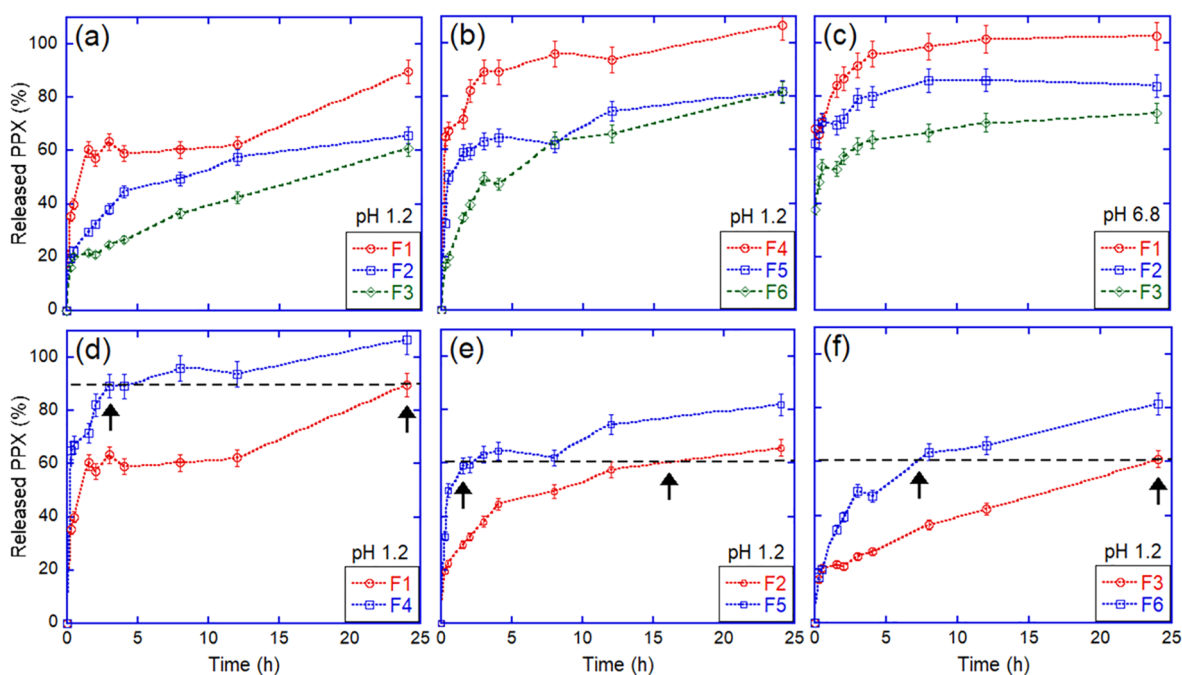

Fig. 7. Release profiles of nanofiber membranes formulations: (a) with PEO/NaHCO$_3$ in pH 1.2 solution; (b) without PEO/NaHCO$_3$ in pH 1.2 solution; (c) with PEO/NaHCO$_3$ in pH 6.8 solution; (d) Eudragit RL <u>only</u> polymer fibers, (e) Eudragit RL and RS (50/50) polymer fibers, and (f) Eudragit RS <u>only</u> polymer fibers in pH 1.2 solution, ($n = 3$).

Table 2
Kinetic model parameters of all formulations.

		First order	Higuchi	Korsmeyer-Peppas	Hixson-Crowell
F1	Eq.	$F = 100 * [1 − Exp(− 0.00257 * t)]$	$F = 2.98 * t^{0.5}$	$F = 24.76 * t^{0.162}$	$F = 100 * [1 − (1–0.000649 * t)^3]$
	r	0.806	0.852	0.963	0.783
F2	Eq.	$F = 100 * [1 − Exp(− 0.00156 * t)]$	$F = 2.27 * t^{0.5}$	$F = 7.64 * t^{0.306}$	$F = 100 * [1 − (1–0.000589 * t)^3]$
	r	0.966	0.960	0.979	0.966
F3	Eq.	$F = 100 * [1 − Exp(− 0.00115 * t)]$	$F = 1.72 * t^{0.5}$	$F = 7.38 * t^{0.257}$	$F = 100 * [1 − (1–0.000227 * t)^3]$
	r	0.943	0.969	0.955	0.940
F4	Eq.	$F = 100 * [1 − Exp(− 0.00844 * t)]$	$F = 4.13 * t^{0.5}$	$F = 43.17 * t^{0.128}$	$F = 100 * [1 − (1–0.001241 * t)^3]$
	r	0.850	0.789	0.992	0.773
F5	Eq.	$F = 100 * [1 − Exp(− 0.003 * t)]$	$F = 3.17 * t^{0.5}$	$F = 28.39 * t^{0.145}$	$F = 100 * [1 − (1–0.0007 * t)^3]$
	r	0.834	0.861	0.897	0.827
F6	Eq.	$F = 100*[1 − Exp(− 0.00218*t)]$	$F = 2.64*t^{0.5}$	$F = 5.77*t^{0.378}$	$F = 100*[1 − (1–0.000589*t)^3]$
	r	0.975	0.966	0.979	0.966

Eq: Equation.
r: Correlation coefficient.

films (F4, F5, F6). A possible explanation for this retarding effect is that when the floating membrane inflates it floats on the dissolution medium and the upper surface is not in contact with the solution. Therefore, the drug release occurs mainly through the bottom surface providing a steady and slow rate. On the other hand, the non-floating membranes are surrounded by the release medium, leading to a faster release. A similar situation was reported in pentoxifylline containing effervescent floating tablets (Elkordy et al., 2015). El-Gibaly also reported that floating chitosan microcapsules showed a retarded release of sodium dioctyl sulfosuccinate compared to non-floating microspheres (El-Gibaly, 2002).

For floating drug delivery systems, no single kinetic model can predict the overall release mechanism, even when the same floating mechanism was utilized. To evaluate drug release kinetics from nanofiber formulations, first-order, Higuchi, Hixson-Crowell, and Korsmeyer-Peppas models were used as below (Eqs. (2)–(5)):

First order model: $F = 100 * [1 − Exp(−k*t)]$ (2)

Higuchi diffusion model: $F = k * t^{0.5}$ (3)

Korsmeyer - Peppas model: $F = k * t^{n}$ (4)

Hixson - Crowell model: $F = 100 * [1 − (1 − k*t)^3]$ (5)

where *F* is the fraction (%) of drugs released in time *t*, *k* is the release rate constant, *n* is the diffusional exponent. In the first order model, the drug release rate is dependent on its concentration (Pawar and Dhavale, 2014). For the Higuchi model, the drug release is proportional to the square root of time, indicating that the drug release is diffusion controlled (Pawar and Dhavale, 2014). The Hixson-Crowell model describes the drug release by dissolution and with changes in the surface area and diameter of the particles (Malana and Zohra, 2013). Finally, the Korsmeyer-Peppas model characterizes the drug release from polymeric systems using different release mechanisms with the *n* value (a drug release exponent), which indicates the mechanism of drug release (Pawar and Dhavale, 2014). If the *n* value is < 0.5, the release is in agreement with a quasi-Fickian diffusion (partial diffusion) mechanism. If the *n* value is between 0.5 and 1.0, the release is controlled by both diffusion and erosion mechanisms. These kinetic models are applied to our release profiles using DDSolver software (Zhang et al., 2010) and summarized in Table 2 with plots given in Fig. S4.

Among the models evaluated, drug release profiles for our formulations were best fitted with the Korsmeyer-Peppas model based on the highest correlation coefficient. PPX diffuses through a Eudragit matrix as a result of structural rearrangements in the polymer support. Based on calculated n values of < 0.5, the release from matrices occurs primarily by diffusion and not by erosion. Eudragit RS and RL

membranes maintained their original shape over the duration of the release tests. Although we produced a floating drug delivery system using uniaxial nanofibers in this study, it might be possible to achieve zero-order drug release profiles using coaxial or triaxial nanofibers with our system (Yu et al., 2015).

4. Conclusions

Nanofibers are gaining in importance in the pharmaceutical field due to their versatile structures and drug delivery capabilities. In this study, we successfully produced pramipexole-loaded nanofibers as the floating drug delivery system embedded with polyethylene oxide/sodium bicarbonate cast films. The release kinetics of incorporated pramipexole can be easily controlled by adjusting the ratio between Eudragit RS and RL. The self-inflating mechanism was successfully demonstrated in the acidic condition and nanofiber pouches have shown more than 72 h total floating time with very small floating lag time. The electrospun nanofiber-based floating gastro-retentive delivery system embedded with a gas generating polyethylene oxide/sodium bicarbonate film provides the sustained release of pramipexole over 24 h. This represents a very attractive alternative to multiple oral dosages for treating various chronic diseases.

CRediT authorship contribution statement

Serdar Tort: Conceptualization, Investigation, Methodology, Formal Analysis, Writing - original draft. **Daewoo Han:** Methodology, Writing - review & editing. **Andrew J. Steckl:** Methodology, Writing - review & editing.

Declaration of Competing Interest

The authors declare that they have no known competing financial interests or personal relationships that could have appeared to influence the work reported in this paper.

Appendix A. Supplementary material

Supplementary data to this article can be found online at https://doi.org/10.1016/j.ijpharm.2020.119164.

References

Adibkia, K., Hamedeyazdan, S., Javadzadeh, Y., 2011. Drug release kinetics and physi-cochemical characteristics of floating drug delivery systems. Expert Opin. Drug Deliv. 8, 891–903. https://doi.org/10.1517/17425247.2011.574124.

Akhgari, A., Tavakol, A., 2016. Prediction of optimum combination of Eudragit RS/ Eudragit RL/ethyl cellulose polymeric free films based on experimental design for using as a coating system for sustained release theophylline pellets. Adv. Pharm. Bull. 6, 219–225. https://doi.org/10.15171/apb.2016.030.

Awasthi, R., Kulkarni, G.T., 2016. Decades of research in drug targeting to the upper gastrointestinal tract using gastroretention technologies: Where do we stand? Drug Deliv. 23, 378–394. https://doi.org/10.3109/10717544.2014.936535.

Bahari Javan, N., Jafary Omid, N., Moosavi Hasab, N., Rezaie Shirmard, L., Rafiee-Tehrani, M., Dorkoosh, F., 2018. Preparation, statistical optimization and in vitro evaluation of pramipexole prolonged delivery system based on poly (3-hydro-xybutyrate-co-3-hydroxyvalerate) nanoparticles. J. Drug Deliv. Sci. Technol. 44, 82–90. https://doi.org/10.1016/j.jddst.2017.11.026.

Baldaniya, L., Saisivam, S., Gohel, M., 2015. Design and evaluation of a novel bio-mimicking in vitro dissolution test apparatus for floating drug delivery systems. Dissol. Technol. 22, 22–28. https://doi.org/10.14227/DT220415P22.

Bani-Jaber, A.K., Alkawareek, M.Y., Al-Gousous, J.J., Abu Helwa, A.Y., 2011. Floating and sustained-release characteristics of effervescent tablets prepared with a mixed matrix of Eudragit L-100-55 and Eudragit E PO. Chem. Pharm. Bull. (Tokyo) 59, 155–160. https://doi.org/10.1248/cpb.59.155.

Darbasizadeh, B., Motasadizadeh, H., Foroughi-Nia, B., Farhadnejad, H., 2018. Tripolyphosphate-crosslinked chitosan/poly (ethylene oxide) electrospun nanofi-brous mats as a floating gastro-retentive delivery system for ranitidine hydrochloride. J. Pharm. Biomed. Anal. 153, 63–75. https://doi.org/10.1016/j.jpba.2018.02.023.

Dwivedi, C., Pandey, I., Pandey, H., Patil, S., Mishra, S.B., Pandey, A.C., Zamboni, P., Ramteke, P.W., Singh, A.V., 2018. In vivo diabetic wound healing with nanofibrous scaffolds modified with gentamicin and recombinant human epidermal growth factor. J. Biomed. Mater. Res. Part A 106, 641–651. https://doi.org/10.1002/jbm.a.36268.

Eberle, V.A., Schoelkopf, J., Gane, P.A.C., Alles, R., Huwyler, J., Puchkov, M., 2014. Floating gastroretentive drug delivery systems: Comparison of experimental and si-mulated dissolution profiles and floatation behavior. Eur. J. Pharm. Sci. 58, 34–43. https://doi.org/10.1016/j.ejps.2014.03.001.

Eisenreich, W., Sommer, B., Hartter, S., Jost, W.H., 2010. Pramipexole extended release: a novel treatment option in Parkinson's disease. Parkinsons. Dis. 2010, 1–7. https://doi.org/10.4061/2010/612619.

El-Gibaly, I., 2002. Development and in vitro evaluation of novel floating chitosan mi-crocapsules for oral use: comparison with non-floating chitosan microspheres. Int. J. Pharm. 249, 7–21. https://doi.org/10.1016/S0378-5173(02)00396-4.

Elkordy, A.A., Abdel Rahim, S., Carter, P., 2015. Design and evaluation of effervescent floating tablets based on hydroxyethyl cellulose and sodium alginate using pentox-ifylline as a model drug. Drug Des. Devel. Ther. 9, 1843–1857. https://doi.org/10.2147/DDDT.S78717.

Elsamaligy, S., Bodmeier, R., 2015. Development of extended release multiple unit ef-fervescent floating drug delivery systems for drugs with different solubilities. J. Drug Deliv. Sci. Technol. 30, 467–477. https://doi.org/10.1016/j.jddst.2015.05.008.

Fukuda, M., Peppas, N.A., McGinity, J.W., 2006. Floating hot-melt extruded tablets for gastroretentive controlled drug release system. J. Control. Release 115, 121–129. https://doi.org/10.1016/j.jconrel.2006.07.018.

Fukui, S., Yano, H., Yada, S., Mikkaichi, T., Minami, H., 2017. Design and evaluation of an extended-release matrix tablet formulation; the combination of hypromellose acetate succinate and hydroxypropylcellulose. Asian J. Pharm. Sci. 12, 149–156. https://doi.org/10.1016/j.ajps.2016.11.002.

Gambhire, M.N., Ambade, K.W., Kurmi, S.D., Kadam, V.J., Jadhav, K.R., 2007. Development and in vitro evaluation of an oral floating matrix tablet formulation of diltiazem hydrochloride. AAPS PharmSciTech 8 (3), E73. https://doi.org/10.1208/pt0803073.

Gianak, O., Pavlidou, E., Sarafidis, C., Karageorgiou, V., Deliyanni, E., 2018. Silk fibroin nanoparticles for drug delivery: effect of bovine serum albumin and magnetic na-noparticles addition on drug encapsulation and release. Separations 5, 25. https://doi.org/10.3390/separations5020025.

Glaessl, B., Siepmann, F., Tucker, I., Rades, T., Siepmann, J., 2010. Mathematical mod-eling of drug release from Eudragit RS-based delivery systems. J. Drug Deliv. Sci. Technol. 20, 127–133. https://doi.org/10.1016/S1773-2247(10)50017-0.

Gryczke, A., Schminke, S., Maniruzzaman, M., Beck, J., Douroumis, D., 2011. Development and evaluation of orally disintegrating tablets (ODTs) containing Ibuprofen granules prepared by hot melt extrusion. Colloids Surfaces B Biointerfaces 86, 275–284. https://doi.org/10.1016/j.colsurfb.2011.04.007.

Hamori, M., Yoshimatsu, S., Hukuchi, Y., Shimizu, Y., Fukushima, K., Sugioka, N., Nishimura, A., Shibata, N., 2014. Preparation and pharmaceutical evaluation of nano-fiber matrix supported drug delivery system using the solvent-based electro-spinning method. Int. J. Pharm. 464, 243–251. https://doi.org/10.1016/j.ijpharm.2013.12.036.

Han, D., Steckl, A.J., 2013. Triaxial electrospun nanofiber membranes for controlled dual release of functional molecules. ACS Appl. Mater. Interfaces 5, 8241–8245. https://doi.org/10.1021/am402376c.

Han, D., Yu, X., Chai, Q., Ayres, N., Steckl, A.J., 2017. Stimuli-Responsive Self-Immolative Polymer Nanofiber Membranes Formed by Coaxial Electrospinning. ACS Appl. Mater. Interfaces 9, 11858–11865. https://doi.org/10.1021/acsami.6b16501.

Hoobakht, F., Ganji, F., Vasheghani-Farahani, E., Mousavi, S.M., 2013. Eudragit RS PO nanoparticles for sustained release of pyridostigmine bromide. J. Nanoparticle Res.

15, 1912. https://doi.org/10.1007/s11051-013-1912-y.

Hu, X., Liu, S., Zhou, G., Huang, Y., Xie, Z., Jing, X., 2014. Electrospinning of polymeric nanofibers for drug delivery applications. J. Control. Release 185, 12–21. https://doi.org/10.1016/j.jconrel.2014.04.018.

Huanbutta, K., Nernplod, T., Akkaramongkolporn, P., Sriamornsak, P., 2017. Design of porous Eudragit ® L beads for floating drug delivery by wax removal technique. Asian J. Pharm. Sci. 12, 227–234. https://doi.org/10.1016/j.ajps.2016.12.002.

Jain, V., Singh, R., 2010. Development and characterization of eudragit RS 100 loaded microsponges and its colonic delivery using natural polysaccharides. Acta Pol. Pharm. - Drug Res. 67, 407–415.

Jenner, P., Könen-Bergmann, M., Schepers, C., Haertter, S., 2009. Pharmacokinetics of a Once-Daily extended-release formulation of pramipexole in healthy male volunteers: Three studies. Clin. Ther. 31, 2698–2711. https://doi.org/10.1016/j.clinthera.2009.10.018.

Jiang, H., Wang, L., Zhu, K., 2014. Coaxial electrospinning for encapsulation and con-trolled release of fragile water-soluble bioactive agents. J. Control. Release 193, 296–303. https://doi.org/10.1016/j.jconrel.2014.04.025.

Jin, M., Yu, D.-G., Geraldes, C.F.G.C., Williams, G.R., Bligh, S.W.A., 2016. Theranostic fibers for simultaneous imaging and drug delivery. Mol. Pharm. 13, 2457–2465. https://doi.org/10.1021/acs.molpharmaceut.6b00197.

Karthikeyan, K., Guhathakarta, S., Rajaram, R., Korrapati, P.S., 2012. Electrospun zein/ eudragit nanofibers based dual drug delivery system for the simultaneous delivery of aceclofenac and pantoprazole. Int. J. Pharm. 438, 117–122. https://doi.org/10.1016/j.ijpharm.2012.07.075.

Lee, Y.-S., Song, J.G., Lee, S.H., Han, H.-K., 2017. Sustained-release solid dispersion of pelubiprofen using the blended mixture of aminoclay and pH independent polymers: preparation and in vitro/in vivo characterization. Drug Deliv. 24, 1731–1739. https://doi.org/10.1080/10717544.2017.1399304.

Li, Y., Wang, D., Lu, S., Zeng, L., Wang, Y., Song, W., Liu, J., 2018. Pramipexole nano-crystals for transdermal permeation: Characterization and its enhancement micro-mechanism. Eur. J. Pharm. Sci. 124, 80–88. https://doi.org/10.1016/j.ejps.2018.08.003.

Malana, M.A., Zohra, R., 2013. The release behavior and kinetic evaluation of tramadol HCl from chemically cross linked Ter polymeric hydrogels. DARU J. Pharm. Sci. 21, 10. https://doi.org/10.1186/2008-2231-21-10.

Malik, R., Garg, T., Goyal, A.K., Rath, G., 2015a. Polymeric nanofibers: targeted gastro-retentive drug delivery systems. J. Drug Target. 23, 109–124. https://doi.org/10.3109/1061186X.2014.965715.

Malik, R., Garg, T., Goyal, A.K., Rath, G., 2015. Diacerein-Loaded novel gastroretentive nanofiber system using PLLA: Development and in vitro characterization. Artif. Cells Nanomed. Biotechnol. 44, 928–936. https://doi.org/10.3109/21691401.2014.1000492.

Mandal, U.K., Chatterjee, B., Senjoti, F.G., 2016. Gastro-retentive drug delivery systems and their in vivo success: A recent update. Asian J. Pharm. Sci. 11, 575–584. https://doi.org/10.1016/j.ajps.2016.04.007.

Misra, S., Pandey, H., Patil, S., Ramteke, P., Pandey, A., 2017. Tolnaftate-loaded poly-acrylateelectrospun nanofibers for an impressive regimen on dermatophytosis. Fibers 5, 41. https://doi.org/10.3390/fib5040041.

Moodley, K., Pillay, V., Choonara, Y.E., du Toit, L.C., Ndesendo, V.M.K., Kumar, P., Cooppan, S., Bawa, P., 2011. Oral drug delivery systems comprising altered geo-metric configurations for controlled drug delivery. Int. J. Mol. Sci. 13, 18–43. https://doi.org/10.3390/ijms13010018.

Muthu, S., Uma Maheswari, J., Srinivasan, S., Isac paulraj, E., 2013. Spectroscopic stu-dies, potential energy surface and molecular orbital calculations of pramipexole. Spectrochim. Acta Part A Mol. Biomol. Spectrosc. 115, 64–73. https://doi.org/10.1016/j.saa.2013.06.004.

Palo, M., Kogermann, K., Laidmäe, I., Meos, A., Preis, M., Heinämäki, J., Sandler, N., 2017. Development of oromucosal dosage forms by combining electrospinning and inkjet printing. Mol. Pharm. 14, 808–820. https://doi.org/10.1021/acs.molpharmaceut.6b01054.

Papadimitriou, S., Bikiaris, D., Avgoustakis, K., Karavas, E., Georgarakis, M., 2008. Chitosan nanoparticles loaded with dorzolamide and pramipexole. Carbohydr. Polym. 73, 44–54. https://doi.org/10.1016/j.carbpol.2007.11.007.

Park, C.G., Kim, E., Park, M., Park, J.-H., Choy, Y. Bin, 2011. A nanofibrous sheet-based system for linear delivery of nifedipine. J. Control. Release 149, 250–257. https://doi.org/10.1016/j.jconrel.2010.10.023.

Pawar, H.A., Dhavale, R., 2014. Development and evaluation of gastroretentive floating tablets of an antidepressant drug by thermoplastic granulation technique. Beni-Suef Univ. J. Basic Appl. Sci. 3, 122–132. https://doi.org/10.1016/j.bjbas.2014.05.005.

Polyvinylpyrrolidone Mw1300 Product Specification [WWW Document], n.d. URL https://www.sigmaaldrich.com/Graphics/COfAInfo/SigmaSAPQM/SPEC/43/437190/437190-BULK_____ALDRICH_.pdf (accessed 9.19.19).

Pawar, S.M., Khatal, L.D., Gabhe, S.Y., Dhaneshwar, S.R., 2013. Establishment of inherent stability of pramipexole and development of validated stability indicating LC-UV and LC-MS method. J. Pharmaceut. Anal. 3 (2), 109–117. https://doi.org/10.1016/j.jpha.2012.07.011.

Qiao, M., Luo, Y., Zhang, L., Ma, Y., Stephenson, T.S., Zhu, J., 2010. Sustained release coating of tablets with Eudragit® RS/RL using a novel electrostatic dry powder coating process. Int. J. Pharm. 399, 37–43. https://doi.org/10.1016/j.ijpharm.2010.07.047.

Reda, R., Wen, M.M., El-Kamel, A., 2017. Ketoprofen-loaded Eudragit electrospun na-nofibers for the treatment of oral mucositis. Int. J. Nanomed. 12, 2335–2351. https://doi.org/10.2147/IJN.S131253.

Reddy, B.V., Navaneetha, K., Sandeep, P., Deepthi, A., 2013. Gastro-retentive drug de-livery system- a review. J. Glob. Trends Pharm. Sci. 4, 1018–1033.

Santocildes-Romero, M.E., Hadley, L., Clitherow, K.H., Hansen, J., Murdoch, C., Colley,

H.E., Thornhill, M.H., Hatton, P.V., 2017. Fabrication of electrospun mucoadhesive membranes for therapeutic applications in oral medicine. ACS Appl. Mater. Interfaces 9, 11557–11567. https://doi.org/10.1021/acsami.7b02337.

Shahriar, S.M.S., Mondal, J., Hasan, M.N., Revuri, V., Lee, D.Y., Lee, Y.K., 2019. Electrospinning nanofibers for therapeutics delivery. Nanomaterials 9, 532. https://doi.org/10.3390/nano9040532.

Shao, H., Fang, J., Wang, H., Lin, T., 2015. Effect of electrospinning parameters and polymer concentrations on mechanical-to-electrical energy conversion of randomly-oriented electrospun poly(vinylidene fluoride) nanofiber mats. RSC Adv. 5, 14345–14350. https://doi.org/10.1039/C4RA16360E.

Shen, X.-X., Yu, D.-G., Zhu, L.-M., Branford-White, C., 2009. Preparation and characterization of ultrafine Eudragit L100 fibers via electrospinning. In: 2009 3rd International Conference on Bioinformatics and Biomedical Engineering. IEEE, pp. 1–4. https://doi.org/10.1109/ICBBE.2009.5163230.

Shen, X., Yu, D., Zhu, L., Branford-White, C., White, K., Chatterton, N.P., 2011. Electrospun diclofenac sodium loaded Eudragit® L 100–55 nanofibers for colon-targeted drug delivery. Int. J. Pharm. 408, 200–207. https://doi.org/10.1016/j.ijpharm.2011.01.058.

Singh, B., 2000. Floating drug delivery systems: an approach to oral controlled drug delivery via gastric retention. J. Control. Release 63, 235–259. https://doi.org/10.1016/S0168-3659(99)00204-7.

Streubel, A., Siepmann, J., Bodmeier, R., 2006. Gastroretentive drug delivery systems. Expert Opin. Drug Deliv. 3, 217–233. https://doi.org/10.1517/17425247.3.2.217.

Suvannasara, P., Praphairaksit, N., Muangsin, N., 2014. Self-assembly of mucoadhesive nanofibers. RSC Adv 4, 58664–58673. https://doi.org/10.1039/c4ra09329a.

Thakral, S., Thakral, N.K., Majumdar, D.K., 2013. Eudragit®: a technology evaluation. Expert Opin. Drug Deliv. 10, 131–149. https://doi.org/10.1517/17425247.2013.736962.

Thapa, P., Jeong, S., 2018. Effects of formulation and process variables on gastroretentive floating tablets with a high-dose soluble drug and experimental design approach. Pharmaceutics 10, 161. https://doi.org/10.3390/pharmaceutics10030161.

Turanli, Y., Tort, S., Acartürk, F., 2019. Development and characterization of methylprednisolone loaded delayed release nanofibers. J. Drug Deliv. Sci. Technol. 49, 58–65. https://doi.org/10.1016/j.jddst.2018.10.031.

Viswanathan, P., Muralidaran, Y., Ragavan, G., 2017. Challenges in oral drug delivery: a nano-based strategy to overcome, in: Nanostructures for Oral Medicine. Elsevier, pp. 173–201. https://doi.org/10.1016/B978-0-323-47720-8.00008-0.

Wang, C., Ma, C., Wu, Z., Liang, H., Yan, P., Song, J., Ma, N., Zhao, Q., 2015. Enhanced bioavailability and anticancer effect of curcumin-loaded electrospun nanofiber. In vitro and in vivo study. Nanoscale Res. Lett. 10, 439. https://doi.org/10.1186/s11671-015-1146-2.

Wang, K., Liu, X.-K., Chen, X.-H., Yu, D.-G., Yang, Y.-Y., Liu, P., 2018a. Electrospun hydrophilic Janus nanocomposites for the rapid onset of therapeutic action of helicid. ACS Appl. Mater. Interfaces 10, 2859–2867. https://doi.org/10.1021/acsami.7b17663.

Wang, Y., Yu, X., Zhang, P., Ma, Y., Wang, L., Xu, H., Sui, D., 2018b. Neuroprotective effects of pramipexole transdermal patch in the MPTP-induced mouse model of Parkinson's disease. J. Pharmacol. Sci. 138, 31–37. https://doi.org/10.1016/j.jphs.2018.08.008.

Yang, C., Yu, D.-G., Pan, D., Liu, X.-K., Wang, X., Bligh, S.W.A., Williams, G.R., 2016. Electrospun pH-sensitive core–shell polymer nanocomposites fabricated using a triaxial process. Acta Biomater. 35, 77–86. https://doi.org/10.1016/j.actbio.2016.02.029.

Yu, D.-G., Li, X.-Y., Wang, X., Yang, J.-H., Bligh, S.W.A., Williams, G.R., 2015. Nanofibers fabricated using triaxial electrospinning as zero order drug delivery systems. ACS Appl. Mater. Interfaces 7, 18891–18897. https://doi.org/10.1021/acsami.5b06007.

Yu, D.-G., Yang, C., Jin, M., Williams, G.R., Zou, H., Wang, X., Annie Bligh, S.W., 2016. Medicated Janus fibers fabricated using a Teflon-coated side-by-side spinneret. Colloids Surf. B Biointerfaces 138, 110–116. https://doi.org/10.1016/j.colsurfb.2015.11.055.

Zhang, Y., Huo, M., Zhou, J., Zou, A., Li, W., Yao, C., Xie, S., 2010. DDSolver: an add-in program for modeling and comparison of drug dissolution profiles. AAPS J. 12, 263–271. https://doi.org/10.1208/s12248-010-9185-1.

Zhou, H., Shi, Z., Wan, X., Fang, H., Yu, D.-G., Chen, X., Liu, P., 2019. The relationships between process parameters and polymeric nanofibers fabricated using a modified coaxial electrospinning. Nanomaterials 9, 843. https://doi.org/10.3390/nano9060843.

Supporting Information

Self-Inflating Floating Nanofiber Membranes for

Controlled Drug Delivery

Serdar Tort [a,b], *Daewoo Han* [a], *and Andrew J. Steckl* [a,*]

[a] Nanoelectronics Laboratory, Department of Electrical Engineering and Computer Science,

University of Cincinnati, Cincinnati, USA 45221-0030

[b] Department of Pharmaceutical Technology, Faculty of Pharmacy, Gazi University, Ankara,
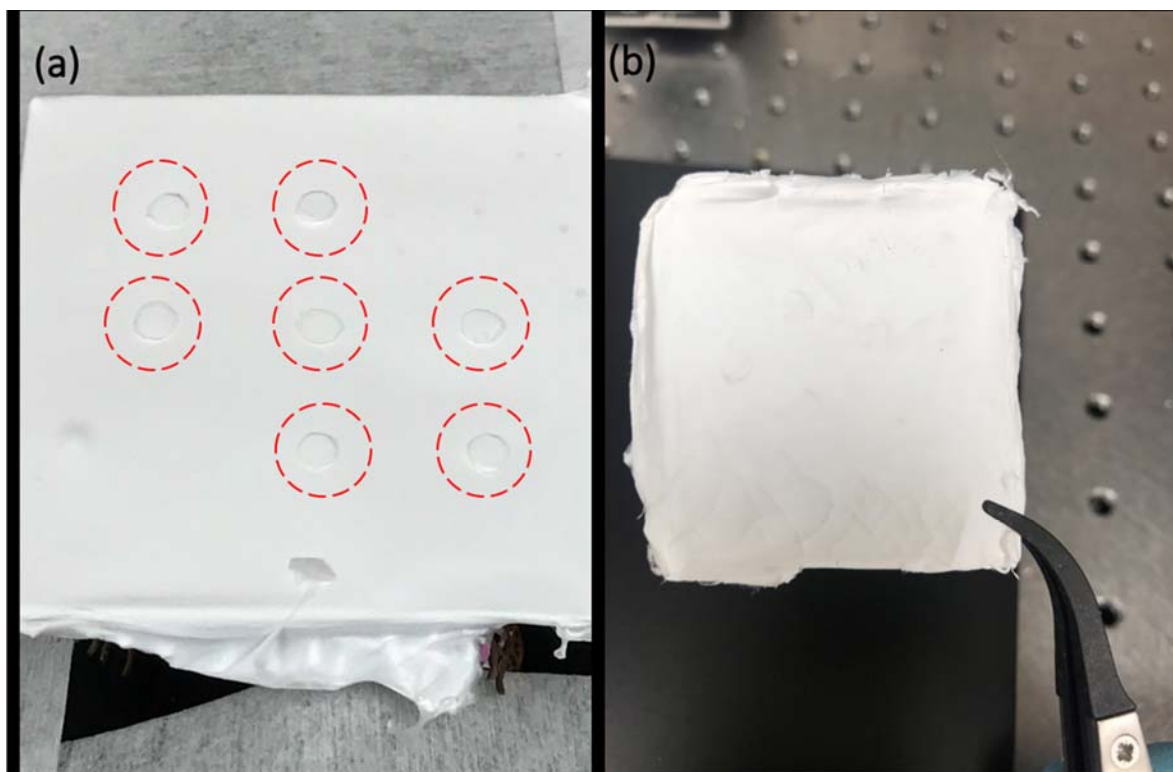
Turkey 06330

[*] Corresponding Author: a.steckl@uc.edu

Fig. S1 Embedding of PEO/NaHCO$_3$ films into nanofibers membranes: (a) placement of PEO/NaHCO$_3$ films (within red circles) on a nanofiber membrane at the mid-point of the electrospinning process; (b) completed nanofiber pouch embedding PEO/NaHCO$_3$ films.
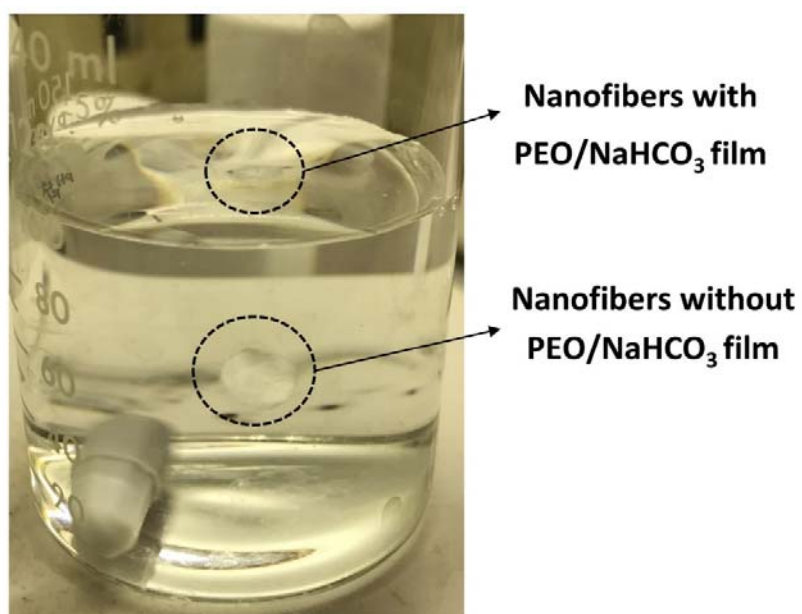
Fig. S2 Comparison of floating properties of nanofibers with and without PEO/NaHCO$_3$ film.
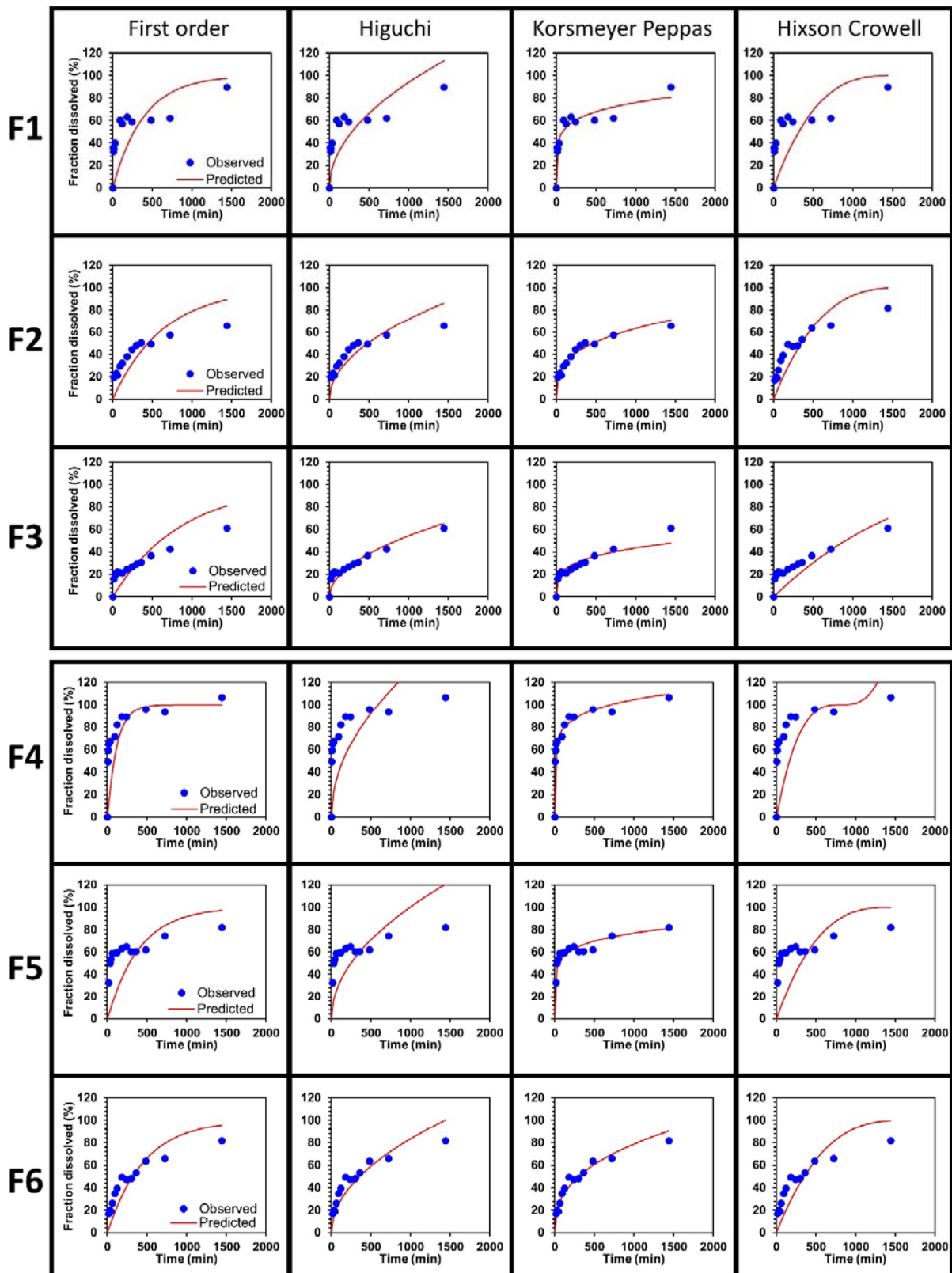
Fig. S3 Release plots of nanofiber formulations and fitting to kinetic models.